The Reliability Information Analysis Center (RIAC) is a DoD Information Analysis Center sponsored by the Defense Technical Information Center

VOLUME 21, NO. 2
DECEMBER 2013

JOURNAL

OF THE RELIABILITY INFORMATION ANALYSIS CENTER

SO, WHO ARE YOU AND WHAT ARE YOU DOING WITH THE RIAC?

David Nicholls, Operations Manager, Reliability Information Analysis Center

To those who have been faithful readers of the *Journal of the Reliability Information Analysis Center* (RIAC) over the last few years, you may recognize that the title of this article sounds somewhat familiar. In the First Quarter, 2006 RIAC Journal, I wrote the article, "So, Who Are You and What Did You Do With the RAC?" (Figure 1), which was published to dispel the after-the-fact confusion that arose out of the re-compete of the old Reliability Analysis Center (RAC) contract. The RAC contract had just been awarded and renamed the RIAC in June 2005 to a new team led by Wyle Laboratories that included Quanterion Solutions Incorporated (which operates the day-to-day RIAC Core functions), the University of Maryland Center for Risk and Reliability (CRR), the Pennsylvania State University Applied Research Laboratory (ARL) and the State University of New York Institute of Technology (SUNYIT). In an instant, 35+ years of Reliability Analysis Center brand recognition and loyalty had been thrown into turmoil and it became necessary for us to jump up and raise our hands to say "Hey, everybody, we're over here!" It took a while for many people to find us again, and in the 8+ years that have transpired since the 2005 RIAC award date, we have been able to successfully enhance and expand our reputation as the recognized DoD Center of Excellence in the Reliability, Maintainability, Quality, Supportability and Interoperability (RMQSI) technical disciplines through many new publications (including the "System Reliability Toolkit," the "Handbook of 217Plus Reliability Prediction Models," "Achieving System Reliability Growth Through Robust Design and Test" and our popular

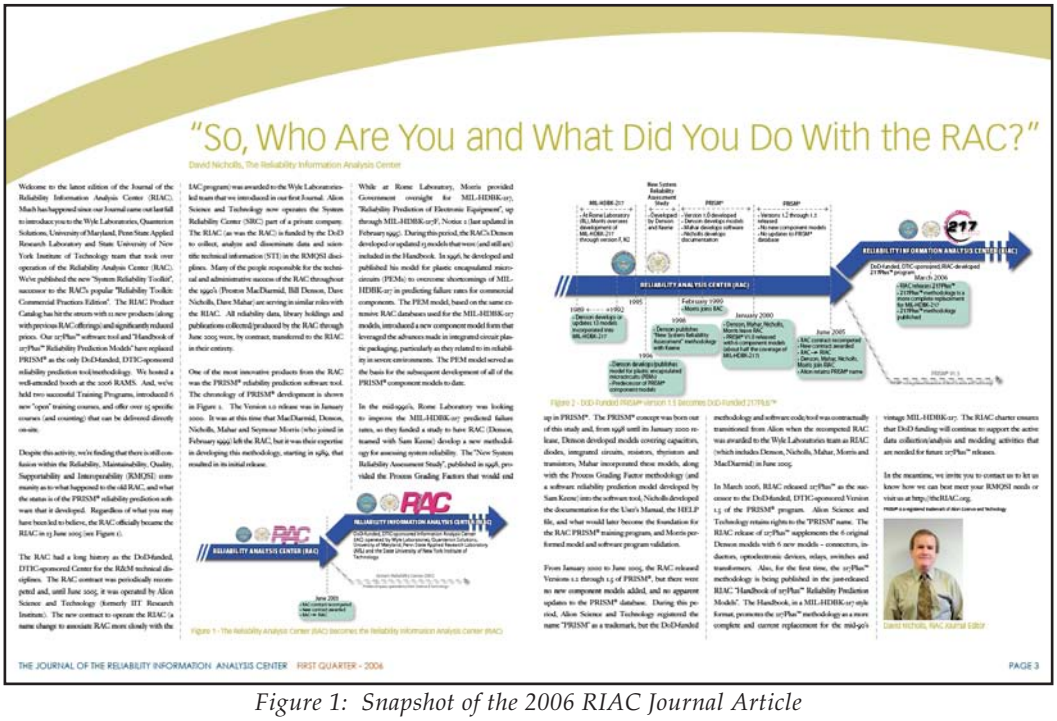

"So, Who Are You and What Did You Do With the RAC?"

David Nicholls, The Reliability Information Analysis Center

Welcome to the latest edition of the Journal of the Reliability Information Analysis Center (RIAC). Much has happened since our Journal came out last fall to introduce you to the Wyle Laboratories, Quanterion Solutions, University of Maryland, Penn State Applied Research Laboratory and State University of New York Institute of Technology team that took over operation of the Reliability Analysis Center (RAC). We've published the new "System Reliability Toolkit", successor to the RAC's popular "Reliability Toolkit: Commercial Practices Edition". The RIAC Product Catalog has hit the streets with 11 new products (along with previous RAC offerings) and significantly reduced prices. Our 217Plus™ software tool and "Handbook of 217Plus™ Reliability Prediction Models" have replaced PRISM® as the only DoD-funded, DTIC-sponsored reliability prediction tool/methodology. We hosted a well-attended booth at the 2006 RAMS. And, we've held two successful Training Programs, introduced 6 new "open" training courses, and offer over 25 specific courses (and counting) that can be delivered directly on-site.

Despite this activity, we're finding that there is still confusion within the Reliability, Maintainability, Quality, Supportability and Interoperability (RMQSI) community as to what happened to the old RAC, and what the status is of the PRISM® reliability prediction software that it developed. Regardless of what you may have been led to believe, the RAC officially became the RIAC in 03 June 2005 (see Figure 1).

The RAC had a long history as the DoD-funded, DTIC-sponsored Center for the R&M technical disciplines. The RAC contract was periodically recompeted and, until June 2005, it was operated by Alion Science and Technology (formerly IIT Research Institute). The new contract to operate the RIAC (a name change to associate RAC more closely with the IAC program) was awarded to the Wyle Laboratories-led team that we introduced in our first Journal. Alion Science and Technology now operates the System Reliability Center (SRC) part of a private company. The RIAC (as was the RAC) is funded by the DoD to collect, analyze and disseminate data and scientific technical information (STI) in the RMQSI disciplines. Many of the people responsible for the technical and administrative success of the RAC throughout the 1990's (Preston MacDiarmid, Bill Denson, Dave Nicholls, Dave Mahar) are serving in similar roles with the RIAC. All reliability data, library holdings and publications (collected/produced by the RAC through June 2005 were, by contract, transferred to the RIAC in their entirety.

One of the most innovative products from the RAC was the PRISM® reliability prediction software tool. The chronology of PRISM® development is shown in Figure 2. The Version 1.0 release was in January 2000. It was at this time that MacDiarmid, Denson, Nicholls, Mahar and Seymour Morris (who joined in February 1999) left the RAC, but it was their expertise in developing this methodology, starting in 1989, that resulted in its initial release.

While at Rome Laboratory, Morris provided Government oversight for MIL-HDBK-217, "Reliability Prediction of Electronic Equipment", up through MIL-HDBK-217F, Notice 2 (last updated in February 1995). During this period, the RAC's Denson developed or updated 13 models that were (and still are) included in the Handbook. In 1996, he developed and published his model for plastic encapsulated microcircuits (PEMs) to overcome shortcomings of MIL-HDBK-217 in predicting failure rates for commercial components. The PEM model, based on the same extensive RAC databases used for the MIL-HDBK-217 models, introduced a new component model form that leveraged the advances made in integrated circuit plastic packaging, particularly as they related to its reliability in severe environments. The PEM model served as the basis for the subsequent development of all of the PRISM® component models to date.

In the mid-1990's, Rome Laboratory was looking to improve the MIL-HDBK-217 predicted failure rates, so they funded a study to have RAC (Denson, teamed with Sam Keene) develop a new methodology for assessing system reliability. The "New System Reliability Assessment Study", published in 1998, provided the Process Grading Factors that would end up in PRISM®. The PRISM® concept was born out of this study and, from 1998 until its January 2000 release, Denson developed models covering capacitors, diodes, integrated circuits, resistors, thyristors and transistors, Mahar incorporated those models, along with the Process Grading Factor methodology (and a software reliability prediction model developed by Sam Keene) into the software tool, Nicholls developed the documentation for the User's Manual, the HELP file, and what would later become the foundation for the RAC PRISM® training programs, and Morris performed model and software program validation.

From January 2000 to June 2005, the RAC released Versions 1.1 through 1.5 of PRISM®, but there were no new component models added, and no apparent updates to the PRISM® database. During this period, Alion Science and Technology registered the name "PRISM" as a trademark, but the DoD-funded methodology and software code/tool was contractually transitioned from Alion when the recompeted RAC was awarded to the Wyle Laboratories team as RIAC (which includes Denson, Nicholls, Mahar, Morris and MacDiarmid) in June 2005.

In March 2006, RIAC released 217Plus™ as the successor to the DoD-funded, DTIC-sponsored Version 1.5 of the PRISM® program. Alion Science and Technology retains rights to the "PRISM" name. The RIAC release of 217Plus™ supplements the 6 original Denson models with 6 new models – connectors, inductors, optoelectronic devices, relays, switches and transformers. Also, for the first time, the 217Plus™ methodology is being published in the just-released RIAC "Handbook of 217Plus™ Reliability Prediction Models". The Handbook, in a MIL-HDBK-217-style format, promotes the 217Plus™ methodology as a more complete and current replacement for the mid-90's vintage MIL-HDBK-217. The RIAC charter ensures that DoD funding will continue to support the active data collection/analysis and modeling activities that are needed for future 217Plus™ releases.

In the meantime, we invite you to contact us to let us know how we can best meet your RMQSI needs or visit us at http://the RIAC.org.

PRISM® is a registered trademark of Alion Science and Technology

David Nicholls, RIAC Journal Editor

THE JOURNAL OF THE RELIABILITY INFORMATION ANALYSIS CENTER FIRST QUARTER - 2006 PAGE 3

Figure 1: Snapshot of the 2006 RIAC Journal Article

NPRD-2011, FMD-2013 and EPRD-2014 reliability databooks), training courses (including a new course addressing reliability growth during system design/development), web-based tools (such as the Web-Accessible Repository of Physics-based Models – WARP), consulting services and direct support to the Warfighter through Technical Area Task (TAT) work.

As the year 2014 arrives, the RIAC is again transforming into a new organization. We thought we would take this opportunity to proactively inform our readership of the changes at hand, and how they will impact the RIAC that you've known for all these years.

The Defense Technical Information Center (DTIC) Director, DoD IACs, Mr. Christopher Zember, writes [Ref. 1]:

> *"The Department of Defense's Information Analysis Centers (IACs) are undergoing the most sweeping change ever undertaken since their inception in 1947, in the wake of the Second World War."*
>
> *"The on-going effort to restructure the IACs will be completed by the summer of 2014. Driven by changes in government policy, while also incorporating best practices gleaned from decades of operational experience, the restructuring of the IACs is intended to accomplish these objectives:*
>
> - *Realign focus to match the top priorities of the Secretary of Defense*
> - *Increase synergy across related technology areas*
> - *Increase opportunities for small businesses*
> - *Lower cost and improve quality through enhanced competition*
> - *Expand the industrial base accessible through the IACs"*
>
> *"A central feature of the IAC model is the establishment of a community of practice for each of the three focus areas of the IACs: Cyber Security and Information Systems, Defense Systems, and Homeland Defense and Security. Through these communities of practice, IACs engage in building and exchanging tacit knowledge, based on the diverse experiences of the individual SMEs within the community. This tacit knowledge goes beyond information contained in formal reports, and has been useful in answering the complex, multidimensional challenges our operational forces face in today's interconnected and dynamic environment."*

Where does the RIAC fit in the new IAC model structure? Figure 2 provides an overview of the transition from the former DTIC IAC structure to the way-ahead.

As highlighted in Figure 3, the functions traditionally performed by the RIAC Core (i.e., the day-to-day operations) will be folded into

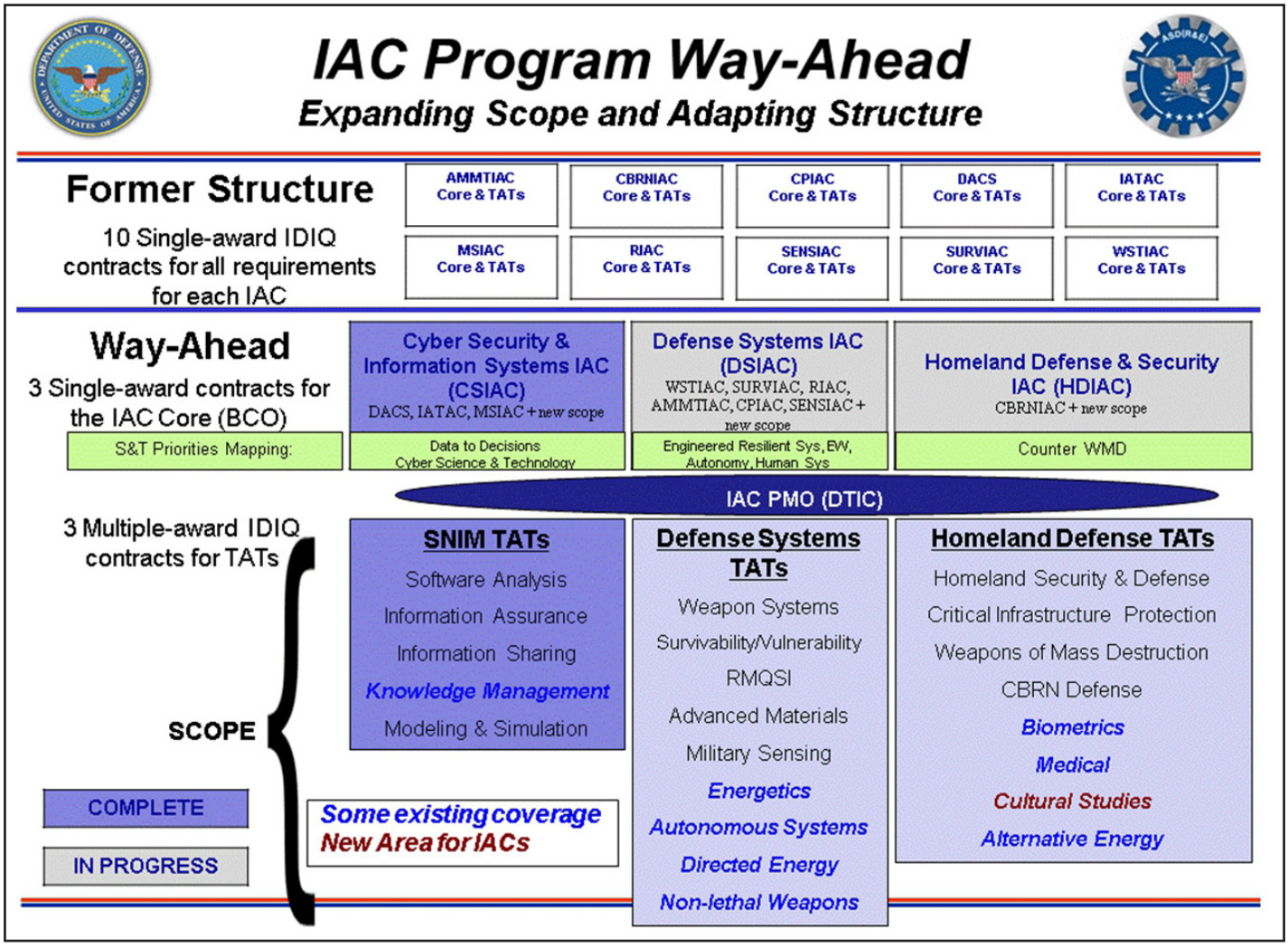

Figure 2: An Overview of the IAC Program Way-Ahead [Ref. 1]

continued on next page ›››

continued from page 3

the Defense Systems IAC (DSIAC) Basic Center Operations (BCO), as will the equivalent Core functions of the Weapons Systems Technology Information Analysis Center (WSTIAC), the Survivability/Vulnerability Information Analysis Center (SURVIAC), the Advanced Materials, Manufacturing, and Testing Information Analysis Center (AMMTIAC), the Chemical Propulsion Information Analysis Center (CPIAC) and the Military Sensing Information Analysis Center (SENSIAC). The individual IAC brands will be phased out as the DSIAC BCO is spun up, but their respective technology areas (RMQSI, in the case of RIAC) will continue to be the major technology focus of the DSIAC operations.[1]

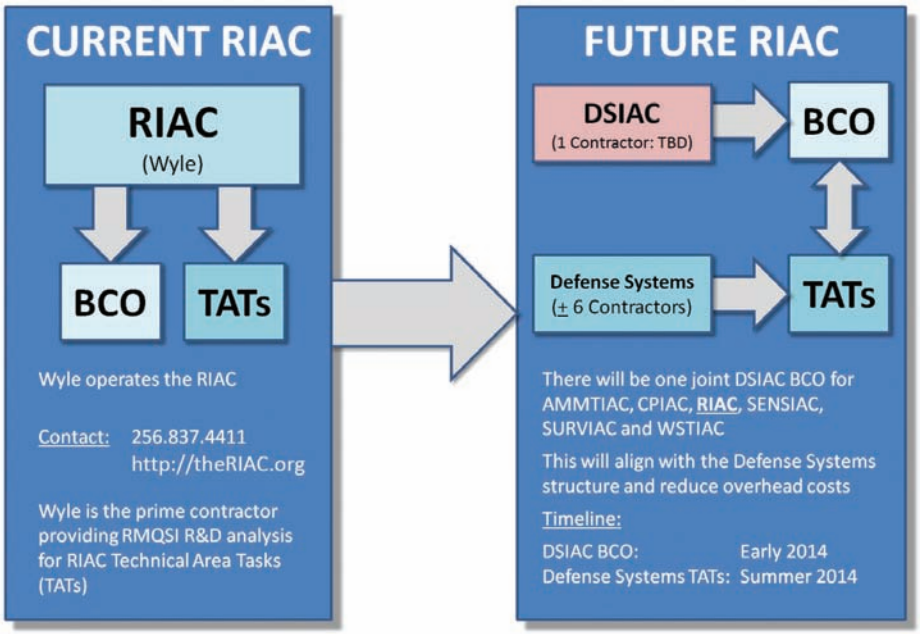

Figure 3: An Overview of the RIAC Way-Ahead [Adapted from http://iac.dtic.mil/way-ahead/pdfs/riac_wayahead.pdf]

A significant difference in the construct of the new IAC model is how TAT work (and the dissemination of STI) will be enhanced by the new role of the BCO. In order to increase competition for TATs, thereby resulting in lower costs to the taxpayer to support Warfighter needs, three separate multiple-award Indefinite Delivery Indefinite Quantity (IDIQ) contract vehicles called Multiple Award Contracts (MACs) are being established for TATs[2] that allow pre-approved contractors to compete for individual TAT work in the specific technical areas covered by the MACs. For the DSIAC TAT MAC, these areas are (1) Weapon Systems, (2) Survivability/Vulnerability, (3) RMQSI (the traditional RIAC charter), (4) Advanced Materials, (5) Military Sensing, (6) Energetics, (7) Autonomous Systems, (8) Directed Energy, and (9) Non-lethal Weapons.

1 At the time this article is being written, the Defense System IAC BCO contract is in competition, with an anticipated award in early 2014.

2 The Software, Networks, Information, Modeling and Simulation (SNIM) TAT contract was awarded on 24 May 2010. At the time this article is being written, the Defense System and Homeland Defense and Security TAT contracts are in competition, with anticipated award dates of Summer 2014 and Winter 2013, respectively.

The process for transferring funds to an IAC MAC (for TATs) or an IAC BCO (for Core Analysis Tasks (CATs)) is fundamentally the same, and is described in more detail on the DTIC website at http://iac.dtic.mil/financial_mgmt.html.

As noted in the Center for Strategic & International Studies (CSIS) DTIC IAC Case Study report [Ref. 2]:

> *"Under the new consolidated, restructured, and enhanced construct, BCOs will be positioned to create and sustain a focus on the Better Buying Power (BBP) Initiative to improve affordability, productivity, and standardization within defense acquisition programs; shape TATs more holistically; and reduce overhead expenses.*
>
> *BCOs still will analyze and synthesize scientific and technical information (STI). However, they also are to take on an expanded role in program analysis and integration by assessing and shaping emerging TATs to ensure consistency with and reduce duplication of prior or other ongoing work and by helping to ensure TATs are more responsive both to customer needs and broader DoD imperatives. BCOs also are to ensure that TAT results are properly characterized, captured, and made available for broad dissemination."*

It is anticipated that the publications, training courses, software tools and services offered by the current RIAC Core operation (and there are over 90 products and 25 training courses) will continue to be available and expanded through the DSIAC BCO to meet the needs of the Defense Systems user community. It should be noted, however, that specific DSIAC BCO offerings will be determined by the government, once the DSIAC contract has been awarded, and will evolve in response to feedback from the user community. RIAC users should continue to actively participate in, and contribute to, the DSIAC community and let your voices be heard regarding your wants, needs and expectations for RMQSI STI under this new IAC model. It is only through your continued and direct support of the DSIAC BCO and MAC that the DoD will be able to acquire, produce and support reliable, sustainable and affordable weapon systems as an integral part of the Better Buying Power initiative.

References

1. Zember, C., "IACs: An Essential Resource for Attaining Better Buying Power," Journal of the Reliability Information Analysis Center, Volume 21, No. 1, August 2013

1. Kiley, G., Powell, G and Livergood, R., "A Case Study for Better Buying Power: Information Analysis Centers of the Defense Technical Information Center," Center for Strategic & International Studies, April 2012

PROBABILISTIC STRUCTURAL HEALTH MONITORING

M. Amiri, V. Ontiveros, A. Keshtgar, M. Nuhi and M. Modarres, Center for Risk and Reliability (CRR), University of Maryland, College Park, MD 20742

Abstract

This paper describes the distinctive features of the probabilistic Structural Health Monitoring (SHM) as implemented at the Center for Risk and Reliability (CRR) at University of Maryland, College Park. Both testing and modeling aspects are briefly described. Particular attention is devoted to the crack initiation and growth modeling in structural materials. Test procedures well suited for detection of microcrack formation and development of probabilistic physics of failure (PPoF) models allowing realistic SHM are included. A brief summary of some of the recent projects accomplished at CRR is introduced.

Introduction

Prevention of premature failure of structures and components is of high priority to ensure reliability and safety. Not only is the enabling technology for realistic prediction of life time important at the design stage, but also for assessment of the integrity and remaining life of a structure or component that has already been in service. Such determinations are vital to avoid premature failures, especially due to the existence of rouge flaws. However, due to a complex spectrum of loading history and changes in environmental, operating and use conditions failure prediction models beg for probabilistic considerations [1]. Therefore, combined mechanism based and probabilistic approach provides a powerful tool for structural integrity assessment.

The Center for Risk and Reliability (CRR) at the University of Maryland (UMD) has recently developed several non-destructive techniques to assess degradation due to creep, fatigue, corrosion-fatigue and pitting failure mechanisms with applications to SHM. Fatigue related models include the use of strain energy, thermodynamic entropy and Acoustic Emission (AE) to estimate crack growth behavior. The experimental data are then utilized to update the degradation model parameters. In what follows we review some of the projects at CRR relevant to SHM.

Acoustic Emission Technique for Crack Growth Rate

Recent developments [2] in testing and probabilistic modeling of macro-crack growth in aluminum structures reveal an intimate connection between AE count rate (dc/dN) and crack growth rate (da/dN) such that

$$\log\left(\frac{da}{dN}\right) = \beta_1 \log\left(\frac{dc}{dN}\right) + \beta_2 \tag{1}$$

where dc/dN is the count rate of AE signals with β_1 and β_2 as the model parameters. A statistical model is developed to describe the relationship between these parameters. Denoting $x_i=\log(dc/dN)_i$ and $y_i=\log(da/dN)_i$, it is assumed that y_i has a normal distribution where both its mean and standard deviation are functions of x_i such that

continued on next page ›››

continued from page 5

$$y_i \sim N(\mu_i, \sigma_i)$$
$$\mu_i = \alpha_1 x_i + \alpha_2$$
$$\sigma_i = \gamma_1 exp(x_i \gamma_2) \quad (2)$$

The unknown parameters (β_1 and β_2) are estimated using hierarchical Bayesian regression and the observed data [2]. A recursive Bayesian inference is used for fusion of AE signals, visual observations and traditional model predictions, for a realistic estimate of crack length. The recursive Bayes model is then used for diagnostic and prognostic purposes by estimating two important SHM quantities: (a) an AE-based instantaneous damage severity index, and (b) an AE-based estimate of the crack length distribution as a function of time, assuming a known initial crack size distribution. Figures 1 and 2 show the experimental setup and the recursive Bayesian estimation of crack size using AE-based and actual measurement (visual observation) of crack growth rate, respectively.

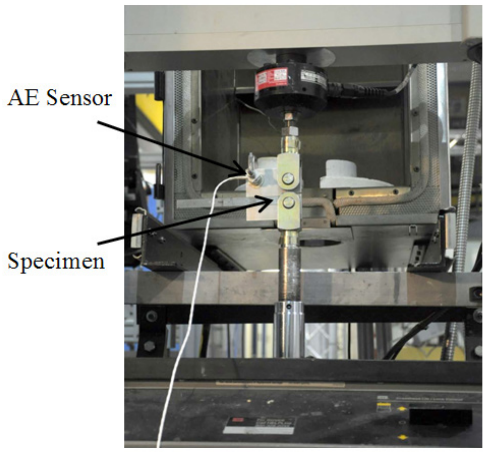

Figure 1. Experimental setup for AE modeling of crack growth (taken from [2] with permission)

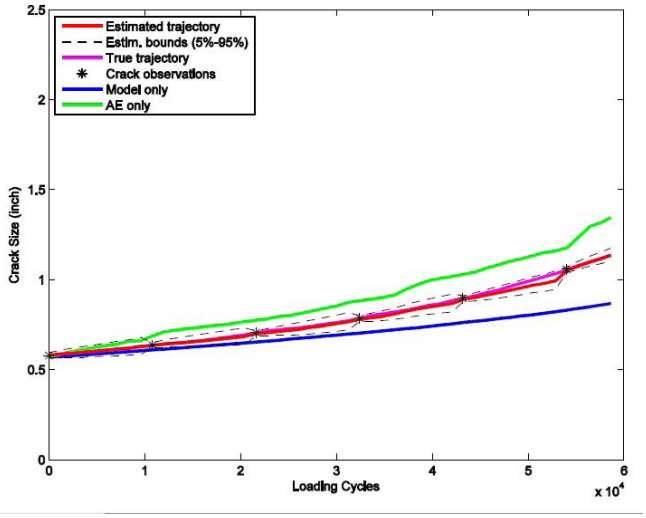

Figure 2. Bayesian estimation of crack size vs. loading cycles (taken from [2] with permission)

Combined Acoustic Emission and Optical Microscopy for Short (micro) Crack Initiation

Ongoing research at CRR aims at developing a probabilistic model for very small (micro) fatigue crack initiation (i.e., micro-cracks which are smaller than 100 microns). The fatigue tests are performed on Al-7075, CT specimens under different loading amplitudes and frequencies. Acoustic emission techniques along with optical microscopy are employed to detect the short crack initiation. A functioning optical microscopy that can take images and record video of surface cracks on the order of 50 microns is under development. The experimental apparatus is shown in Figure 3. The objective of this research is that the time of micro-crack initiation is correlated to the AE features such as the signal count, energy, rise time and amplitude. Figure 4 shows that an intimate correlation exists between the occurrence of the first AE event and incipient fatigue cracking. Our research shows that the first observation of surface cracks occurs after detection of the first high amplitude AE event as shown in Figure 4. For example in this figure, the first AE event was recorded at *N*=18500 cycles while the first observable crack of size of 68 micron was detected at *N*=30840 cycles.

A literature review shows evidence of such a correlation [3], however, many challenging questions must be addressed. For example, as the specimen thickness and geometry changes, how do the AE features change? Optical microscopy techniques used in this research can only reveal surface damage, while AE signals are generated throughout the entire thickness of the specimen (i.e., includes subsurface micron-level crack formation). Therefore, it is highly possible that the AE signals would detect incipient crack formations prior to the crack observation by optical microscopy. Other questions include, how do the AE features change in the presence of friction emission? Friction emission is related to the grating between existing fracture surfaces. How can a prediction model address crack formation when the specimen undergoes a series of variable amplitude loading (and/or overloads)?

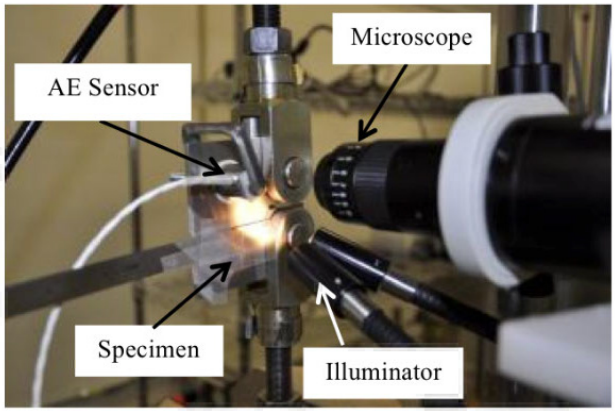

Figure 3. Experimental setup for combined AE-Microscopy for short crack detection

continued on next page ›››

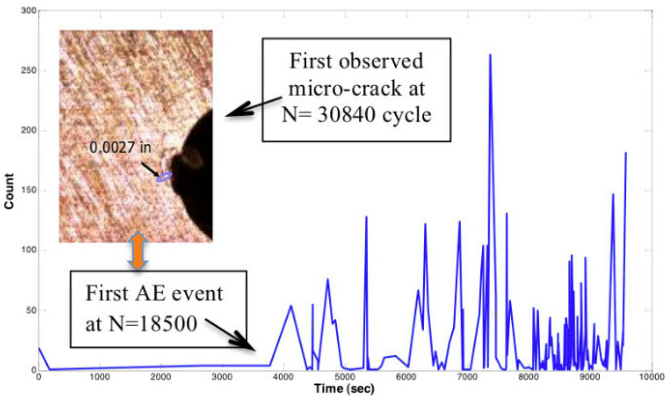

Figure 4. Number of AE counts per cycle vs. time

Thermodynamic Entropy Generation Approach to Crack Initiation

Research shows that fatigue is accompanied by hysteresis-type dissipation of energy that tends to degrade the system and raise its entropy [4]. Production of entropy is the cause of increasing internal damage in the material that causes degradation and aging. Typically, the energy dissipated in a material subject to cyclic loading manifests itself as heat and causes an increase in temperature. Experiments show [4] that particularly when metals are subjected to high-stress cyclic fatigue testing, the temperature rises. Thus, the establishment of a relationship between thermodynamic entropy and failure of structure has become a subject of considerable interest.

Ongoing research at the CRR is aimed at the development of fatigue (micro) crack initiation and growth modeling via the concept of entropy—the most important quantitative metric of disorder—and determination of its link to damage. In this research we investigate whether the thermodynamic entropy can effectively address the mechanism of crack initiation. During each fatigue cycle, plastic work and strain energy are dissipated as a fatigue crack forms and entropy, s_i, is generated at the rate of [5]:

$$\dot{s}_i = \frac{1}{T}\boldsymbol{\sigma}:\dot{\boldsymbol{\varepsilon}}_p - \frac{1}{T}A_k\dot{V}_k - \frac{1}{T}Y\dot{D} - \frac{1}{T^2}\boldsymbol{q}\cdot\nabla T \qquad (3)$$

where σ is the stress tensor, $\dot{\boldsymbol{\varepsilon}}_p$ is the plastic strain rate, T is absolute temperature, V_k can be any internal variable such as hardening, A_k are thermodynamic forces associated with the internal variables, D is the damage variable, Y is the thermodynamics force associated with damage variable, and $\boldsymbol{q}$ is the heat flux. Integration of Eq. (3) from beginning of the test to the time (or equivalent cycle) of crack initiation represents the accumulation of thermodynamic entropy for crack initiation.

Figure 5 shows the results of entropy accumulation for crack initiation of Aluminum 7075-T6 undergoing axial fatigue test. The accumulated entropy was found to vary from 0.2 to 0.37 (MJ/m^{3}K) with an average of 0.29 (MJ/m^{3}K). It is hypothesized that the accumulated thermodynamic entropy generation up to crack initiation is a material constant independent of load and frequency. Therefore, a crack forms in a material upon gaining a certain entropy generation. The scatter observed in the data is associated with the fact that the samples were visually inspected for crack initiation and there was an uncertainty in detecting cracks at the early stage of initiation.

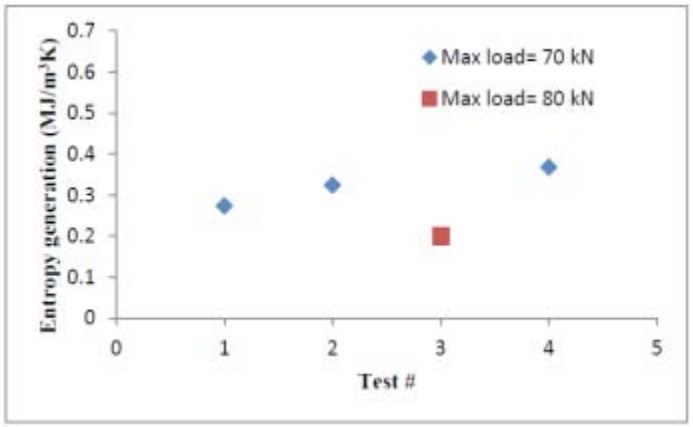

Figure 5. Entropy generation for crack initiation

Creep Failure Mechanism

Creep is one of the most critical failure modes commonly observed in high-temperature operating components in power plants, chemical plants and oil refineries. It is generally referred to as an excessive plastic deformation of material at high temperatures under constant load. Creep degradation occurs during an extended period of time and usually starts by initiation and propagation of microdefects. Research at the CRR has been carried out to develop a probabilistic model capable of capturing the entire creep curve (with only two major parameters, represented by probability density functions) [6]. Two materials, Aluminum 7075-T6 and carbon steel X-70, are considered. For Al 7075-T6, temperature ranges from 405°C to 430°C with stress ranging from 460 MPa to 520 MPa. These ranges for X-70 carbon steel are 410°C to 500°C and 133 MPa to 620 MPa, respectively. Figure 6 shows the experimental apparatus used for creep test.

A creep model is developed in the following form that accounts for stress and temperature dependencies in the entire region of creep progression:

$$\varepsilon_c = A.t^n + B.t^m\, exp(p.t) \qquad (4)$$

where ε_c is creep strain, t is time, A, B, n, m and p are material parameters dependent on stress and temperature [6]. A Bayesian updating framework is used to estimate model parameters A and B in Eq. (4). Prior estimates for A and B are taken from generic creep data

continued on next page ›››

continued from page 7

available in the literature. A lognormal distribution was assumed to represent the variability of creep strain, the likelihood function of the creep strain and the corresponding different percentiles of this distribution as:

$$f(\varepsilon_i)=LN(\mu_i,s_i) \quad (5)$$

where μ_i and s_i are the log-mean and log-standard deviation of the strain distribution. The log-mean of the strain distribution is expressed as:

$$\mu_i=LN[A.t^n+B.t^m\ exp(p.t)] \quad (6)$$

A Windows-based Markov Chain Monte Carlo program (WinBUGs) platform was then used for estimating posterior distributions of parameters A and B. Figure 7 shows the creep curves of X-70 carbon steel at different temperatures. In this figure, for example, 0.04% strain at 450°C is taken as the critical level of inspection. Therefore, the probability of exceedance (amount of failure accumulation) above 0.04% strain is highlighted at different times.

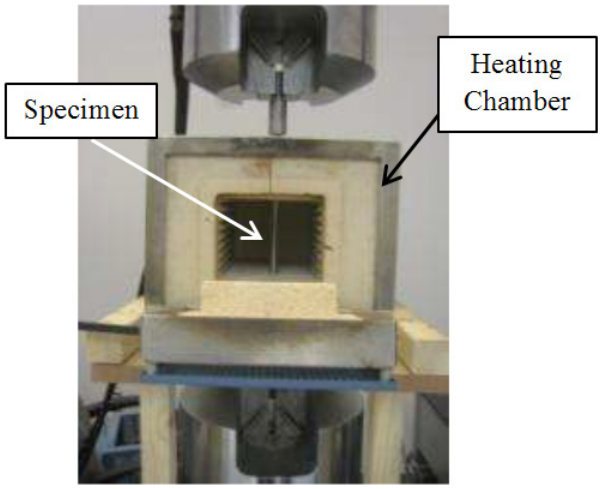

Figure 6. Test setup for creep test (taken from [6] with permission)

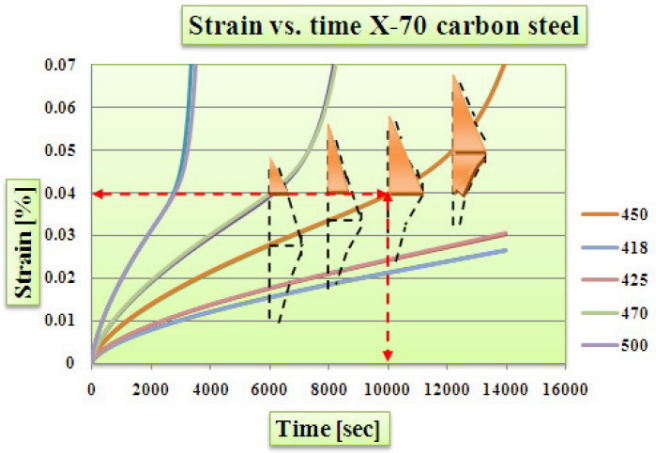

Figure 7. Creep curves for X-70 carbon steel at different temperatures (taken from [6] with permission)

Pitting and Corrosion-Fatigue of Piping

Generally, corrosion is referred to as degradation caused by long term exposure of metals to corrosive media. Consequences of failure are usually catastrophic and costly. The combined effect of stress and corrosion is a common mode of failure observed in pipelines conveying high-pressure corrosive chemical agents. Multi-year research has been performed at CRR for prognostic health management of structures subjected to pitting and carrion-fatigue [7]. In this research an empirical probabilistic model is developed for pitting-corrosion and corrosion-fatigue of X-70 carbon steel used in oil pipelines. The model parameters are estimated through a Bayesian inference from test data. The experimental setup is shown in Figure 8.

The Journal of the Reliability Information Analysis Center is published quarterly by the Reliability Information Analysis Center (RIAC). The RIAC is a DoD Information Analysis Center (IAC) sponsored by the Defense Technical Information Center (DTIC) and operated by a team led by Wyle Laboratories, and including Quanterion Solutions Incorporated, the Center for Risk and Reliability at the University of Maryland, the Penn State University Applied Research Lab (ARL) and the State University of New York Institute of Technology (SUNYIT).

The Reliability Information Analysis Center
100 Seymour Road
Suite C101
Utica, NY 13502-1311
Toll Free: 877.363.RIAC (7422)
P 315.351.4200 // FAX 315.351.4209
inquiry@theRIAC.org
http://theRIAC.org

RIAC Journal Editor, David Nicholls
Toll Free: 877.363.RIAC (7422)
P 315.351.4202 // FAX 315.351.4209
dnicholls@theRIAC.org

Glenda Smith
RIAC Contracting Officer's Representative,
Defense Technical Information Center
P 703.767.9113
gsmith@dtic.mil

Joseph Hazeltine
RIAC Director,
Technical Area Task (TAT) Manager
P 256.922.6936 // FAX 256.922.4243
joseph.hazeltine@wyle.com

Preston MacDiarmid
RIAC Technical Director
Toll Free 877.808.0097
P 315.732.0097 // FAX 315.732.3261
pmacdiarmid@quanterion.com

Kim Austin
RIAC Deputy Director TATs/SAs
P 301.863.4466 // FAX 301.866.2292
kim.austin@wyle.com

David Nicholls
RIAC Operations Manager
Toll Free 877.363.RIAC (7422)
P 315.351.4202 // FAX 315.351.4209
dnicholls@theRIAC.org

David Mahar
Software & Database Manager
Toll Free 877.808.0097
P 315.732.0097 // FAX 315.732.3261
dmahar@theRIAC.org

Patricia Smalley
RIAC Training Coordinator
Toll Free 877.363.RIAC (7422)
P 315.351.4200 // FAX 315.351.4209
psmalley@theRIAC.org

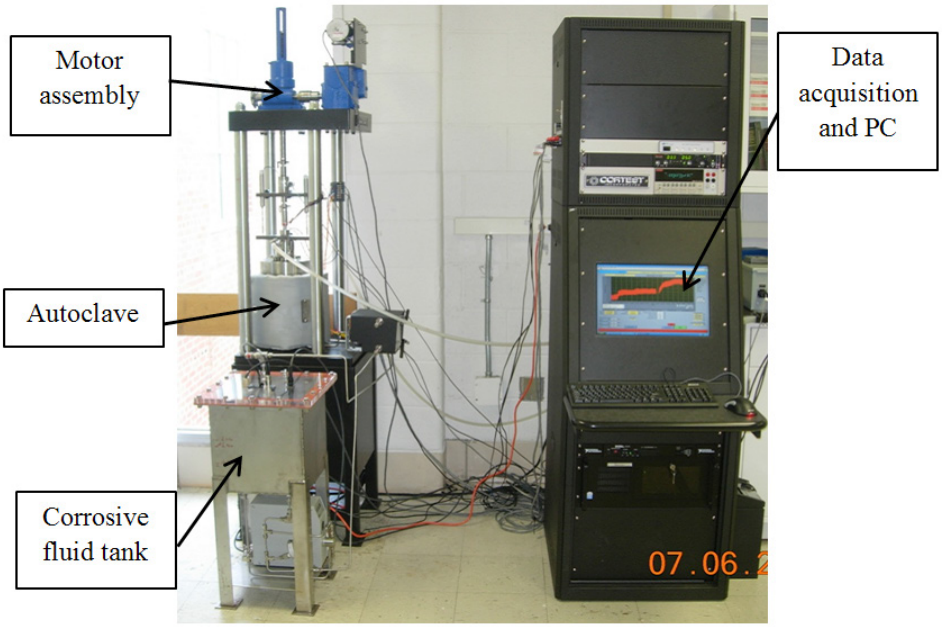

Figure 8. Test setup for corrosion-fatigue testing

A model is proposed to predict the remaining life of the pipeline subjected to pitting and corrosion-fatigue. The model relies on prediction of crack length as:

$$a=C_1 N^{1/3}+C_2 N^2 \exp(0.4545\times10^{-5} N) \quad (7)$$

where a is the crack length (treated as a lognormal distribution), N is the number of fatigue cycles, C_1 and C_2 are parameters dependent on stress, frequency and concentration of chemical agents. The first term in Eq. (7) denotes crack length due to pitting corrosion and the second term represents the corrosion-enhanced fatigue crack growth [7]. The parameters of the model are represented by the probability density functions and estimated through a Bayesian approach based on the test data. Figure 9 schematically shows crack length versus number of cycles for different stresses and concentrations.

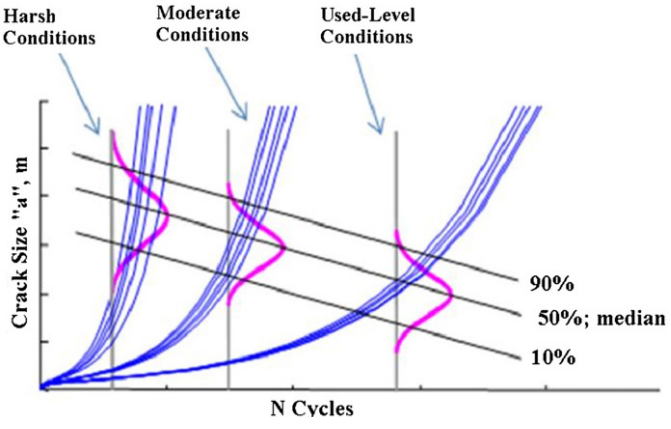

Figure 9. Distribution of crack size (taken from [7] with permission)

Concluding Remarks

In this paper, we reviewed some of the recent research projects accomplished at the CRR relevant to Structural Health Monitoring. Some of the projects are still ongoing at this center. Both experimental and modeling capabilities were discussed. In summary, some of the projects can be listed as:

- Acoustic emission approach to fatigue crack propagation
- Combined optical microscopy and acoustic emission modeling of fatigue short crack initiation
- Thermodynamic entropy approach to fatigue crack initiation
- Creep failure of pipelines
- Pitting and corrosion-fatigue of pipelines

These projects aim at developing probabilistic failure prediction models based on the Bayesian estimation approach. More specifically, we are interested in degradation model updating at any point in time based on all available sources of information (sensors, visual observations, etc.) from test data.

References:

1. Modarres, M., Kaminskiy, and M., Krivtsov, V., "*Reliability engineering and risk analysis: A practical guide*," Marcel Dekker, New York, 1999
2. Rabiei, M., "A Bayesian framework for structural health management using acoustic emission monitoring and periodic inspection," PhD Dissertation, University of Maryland, College Park, 2011
3. Kohn, D.H., Ducheyne, P., and Awerbuch, J., "Acoustic emission during fatigue of Ti-6Al-4V: Incipient fatigue crack detection limits and generalized data analysis methodology," *Journal of Materials Science*, Vol. 27, pp: 3133-3142, 1992.
4. Khonsari, M.M., and Amiri, M., "*Introduction to Thermodynamics of Mechanical Fatigue*," CRC Press, Taylor & Francis Group, Boca Raton, FL, 2012
5. Lemaitre, J., and Chaboche, J.-L., "*Mechanics of Solid Materials*," Cambridge University Press, Cambridge, UK, 2000
6. Nuhi, M., "Classification and probabilistic model development for creep failures of structures: Study of X-70 Carbon Steel and 7075-T6 Aluminum alloys" MSc Thesis, University of Maryland, College Park, 2011
7. Chookah, M., Nuhi, M., and Modarres, M., "A probabilistic physics-of-failure model for prognostic health management of structures subject to pitting and corrosion-fatigue," *Reliability Engineering and System Safety*, Vol. 96, pp: 1601–1610, 2011

FROM THE TITANIC TO ULTRASONIC WAVES IN SOLID MEDIA

Clark Moose, Pennsylvania State University Applied Research Laboratory
Jason Bostron, Pennsylvania State University PhD Candidate

Ultrasound was developed as a viable detection tool in the early decades of the 20th century in response to the sinking of the Titanic, and developed further with the advent of submarine warfare in World War I. By the 1930s, ultrasound was being expanded to encompass metal flaw detection and for medical uses, primarily as therapy rather than for imaging. Hundreds of researchers over the next half century worked to improve the materials and techniques of ultrasound for both inspection and medical imaging, with several notable advances contributed by Penn State materials scientists, especially in the field of piezoelectrics.

Another key development pioneered at Penn State is the use of ultrasonic guided waves in nondestructive testing and structural health monitoring. "This is a breakthrough," says Prof. Joseph Rose, an internationally recognized expert on ultrasonics for nondestructive testing. "If they were going to inspect a buried pipeline in the old days, they would have to dig it up and take an ultrasonic transducer and look point by point around the circumference and along the length. It would take days to see if there was any corrosion, wall thinning, or cracking."

Though the principles of guided waves and some of the mathematics behind them were worked out by the early part of the 20th century, the field had to wait until the advent of fast computers to fully understand and utilize guided waves. Much of that work was done in Rose's group, which remains the leader in ultrasonic guided wave methods. Rose's textbook, *Ultrasonic Waves in Solid Media* (1999), has been used at MIT, Stanford, Georgia Tech, and by engineers around the world.

Bulk wave versus guided wave

To understand the difference between the bulk ultrasonic waves and the new guided wave method of inspection, imagine pointing a flashlight straight down onto a tabletop from a few inches away and moving the small circle of light back and forth across the entire tabletop looking for a flaw. Not only is this process too slow, but it could easily skip a section and thereby miss a defect. Think of this method as the equivalent of standard bulk wave inspection. Guided waves, on the other hand, are like laying the flashlight on its side and sweeping the light parallel to the tabletop. An illustration of the coverage area in a plate is shown in Figure 1.

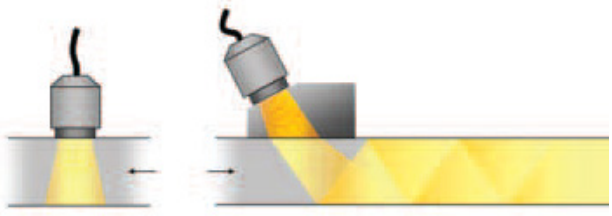

Figure 1. Illustration of bulk wave versus guided wave ultrasonic inspection.

"Guided wave inspection is fast, it's easy to do, and the place where you set your sensors is not so critical," says Rose. And most significantly for the nation's failing infrastructure, guided wave ultrasound can reach into hidden places – underground, behind walls, underneath paint and corrosion, or buried in concrete. As long as one point is accessible, guided waves can detect the problem and pinpoint its location.

In the U.S. alone there are millions of miles of pipelines carrying everything from water to crude oil. Rose's group developed an ultrasonic guided wave focusing technique that is now being used around the world for pipeline inspections, as depicted in Figure 2. The technique can send ultrasonic energy for potentially hundreds of feet along a pipe and focus the energy at any point. This technique could prevent future environmental disasters such as the one in which a burst pipe dumped 800,000 gallons of heavy crude oil into the Kalamazoo River system in Michigan of July 2010.

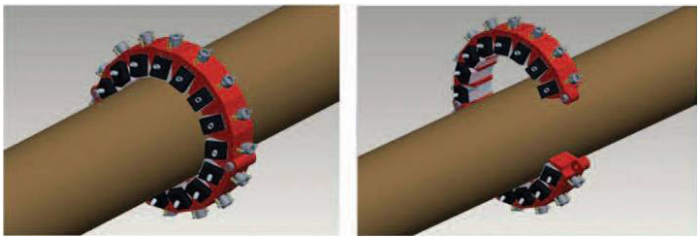

Figure 2. A typical wrap around ultrasonic guided wave sensor arrangement for long range ultrasonic guided wave inspection of piping.

High speed technology transfer

The trip from university laboratory to industrial production is so fraught with failure that it has become known as the Valley of Death. It is not unusual for technology transfer from lab to industry to take ten to twenty years to be adopted. That has not been the case with guided waves, where the technologies being developed in the lab today will likely be in use in the field within the space of a year or two, Rose notes. He suggests that the reason for the fast acceptance of the new ultrasound technology is its ability to solve problems that previously had no solution.

One such problem is train derailments caused by transverse cracking in the rail head, the part of the rail that the wheel runs on. Rail heads can become stressed under the heavier loads that modern freight trains carry, causing the most common type of catastrophic rail failure. Although the current method of bulk wave inspection can find many less serious defects in rails, it cannot easily see vertical transverse cracks below the surface because the energy does not reflect back to the surface. Using guided waves, rather than sending energy from the surface down to the base, the energy is sent downstream several feet in the railhead and vertical cracks are easily detected. "Normal inspection techniques can't do anything beneath the rough surface of the rail head," Rose explains, "but the ultrasound guided energy sneaks under the rough surface and looks at the defects inside the rail head, and even in the web and the base."

Fundamentals

A comparison of ultrasonic bulk waves with ultrasonic guided waves is illustrated in Figure 3. Note that bulk waves cover only a small localized section of a structure. Scanning is necessary to complete an inspection of a test part. The ultrasonic guided wave floods a large area from a single probe position. Two basic guided wave excitation examples include angle-beam excitation and comb excitation as illustrated in the bottom half of Figure 3. A more detailed comparison is presented in Table 1.

Ultrasonic guided waves can be used to inspect almost any structure since the structures fall into a class of natural wave guides, such as plates (aircraft skin, marine structures), rods (cylindrical, square, rail, etc.), hollow cylinders (pipes, tubing), multi-layer structures, curved/flat surfaces on a half-space, multiple layers on a half space or even discrete interfaces. Again, widespread adaptation of guided waves has occurred because of improvements in understanding and in signal interpretation. A special challenge, however, is on thick sections, but even here, surface waves can be used to inspect regions close to the surface of a structure. Frequency changes can increase the depth of penetration and hence improve the examination of a structure.

The many exciting benefits of ultrasonic guided waves are: (1) inspection over long distances from a single transducer position; (2) the ability to inspect hidden structures and structures under water, coatings, soil, insulations and concrete; and (3) cost effectiveness due to inspection simplicity and speed. These reasons have propelled the development of guided waves forward. Additionally, site preparation for inspection is greatly reduced as a result of large coverage of hidden sections of a structure.

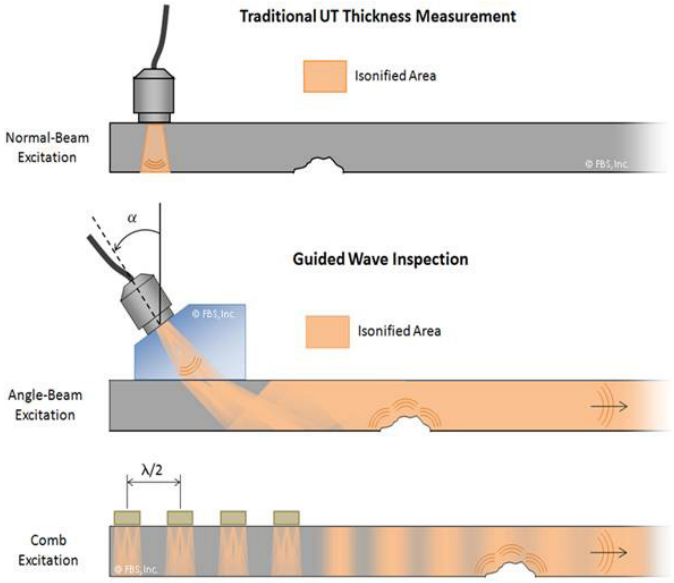

Figure 3. Comparison of ultrasonic bulk and guided waves.

Table 1. A Comparison of the Currently Used Ultrasonic Bulk Wave Technique and the Ultrasonic Guided Wave Inspection Procedure.

Bulk Wave	Guided Wave
Tedious and time consuming	Fast
Point by point scan (rectangular grid scan)	Global in nature (approximate line scan)
Unreliable (can miss points)	Reliable (volumetric coverage)
High level training required for inspection	Minimal training
Fixed distance from area of concern required	Any reasonable distance from defect acceptable
Defect must be accessible and area seen	Defect can be hidden

continued on next page ›››

continued from page 11

Let us now consider some aspects of wave mechanics associated with guided waves. For every wave guide there is a unique set of phase velocity dispersion curves as shown in the left graph of Figure 4 for a particular structure. Group velocity dispersion curves can be calculated from the phase velocity dispersion curves. Attenuation dispersion curves can be calculated from computed complex roots in the eigenvalue problem. The group velocity is the speed at which the wave travels in the physical structure and the attenuation is the amount of energy lost per distance traveled.

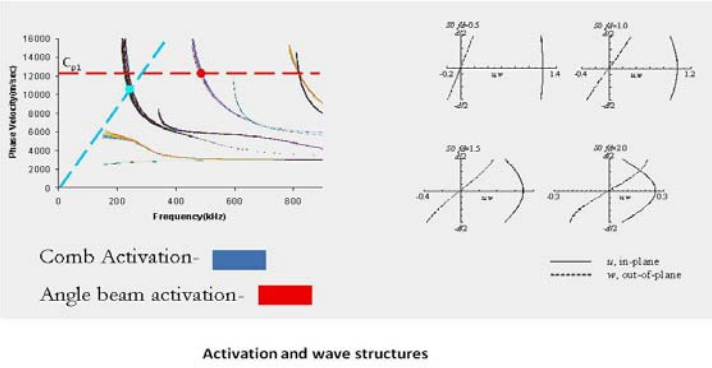

Figure 4. Example phase velocity dispersion curves and activation (left) and wave structure (right).

For every point on the dispersion curve there is a corresponding wave structure that is a special distribution across the thickness of the structure of such variables as in-plane displacement and out of plane displacement, as shown in the right side of Figure 4. Note for example, that if the outer surface has dominant out of plane displacement, a water-loaded plate would lead to ultrasonic energy leakage into the fluid. On the other hand, if the outer surface had only in-plane displacement, the ultrasonic guided wave energy propagating in the plate would not see the fluid. Other variables like shear stress, normal stress, or energy could also be considered. In fact, the key to success in ultrasonic guided wave experiments is associated with a wise choice of mode and frequency on the dispersion curve.

The experimental ability to get onto a dispersion curve is possible by using a comb activation line or angle beam activation line as demonstrated in the left side of Figure 4. To do this, of course, sufficient frequency bandwidth within a transducer is required to be successful. A further challenge is trying to select a proper mode and frequency. Because of the excitation transducer's source influence (size and vibration pattern) there will be a phase velocity spectrum along with the frequency spectrum. The activation region in the phase velocity dispersion curve space is quite large; hence many modes and frequencies are generated at the same time. Proper sensor design and narrow band frequency content can improve the result.

We will now consider the modeling analysis component associated with the understanding of ultrasonic guided waves. The scientific approach makes use of a Hybrid Analytical-FEM computation strategy illustrated in Figure 5. The FEM computation process is useless unless proper boundary conditions are considered in a simulation of an ultrasonic guided wave inspection. The boundary condition comes from a sensor design that comes from a choice of appropriate wave structure from the phase velocity/dispersion curve space, hence an appropriate mode and frequency choice to solve a particular NDE problem.

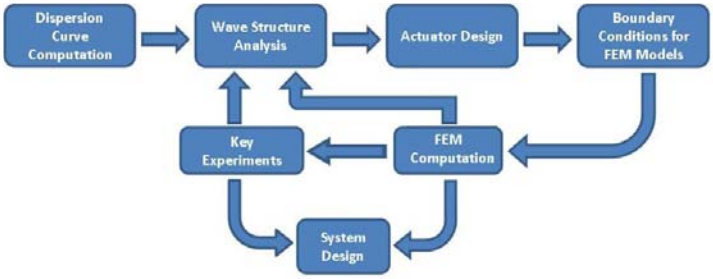

Figure 5. The Hybrid Analytical FEM Approach for Solving Guided Wave Problems

A few sample problems that have been solved using the Hybrid Analytical-FEM computation strategy include:

- Rail – transverse cracking under shelling, defect in base
- Adhesive Bonding – weak interface
- Water-Loaded Structure – to avoid false alarms
- Gas Entrapment – leaky and non-leaky waves
- De-icing – maximum shear stress at the interface
- Piping – flexural mode as the best selection for focusing

In this brief overview, we've shown how the strong advances in guided wave understanding and computational power are making guided wave inspections a reality today. Of particular significance are NDE applications in aircraft, pipelines, rails, bridges, marine structures and other geometries that form natural wave guides for propagating ultrasound.

References (excerpts from):

1. J.L. Rose, *Ultrasonic Waves in Solid Media*, Cambridge University Press, 1999.
2. J.L. Rose, "The Upcoming Revolution in Ultrasonic Guided Waves" (Plenary Paper), *Nondestructive Characterization for Composite Materials, Aerospace Engineering, Civil Infrastructure and Homeland Security 2011*, edited by H. Felix Wu, Proc. of SPIE Vol. 7983, 2011.

Acknowledgment:

The authors wish to express their appreciation for support of this effort by the Office of Naval Research (ONR), whose Navy Manufacturing Technology Program Center of Excellence (Institute for Manufacturing and Sustainment Technologies—iMAST) provided the foundation within this area of research. Any opinions, findings, conclusions and recommendations expressed in this material are those of the author and do not necessarily reflect the views of the Department of Defense or the United States Navy.

The authors also wish to extend their appreciation to Joseph L. Rose, Ph.D., who is the Paul Morrow professor of engineering design and manufacturing at the Pennsylvania State University, for his support in preparing this article.

PRACTICAL SOLUTIONS TO QUANTITATIVE RELIABILITY PROBLEMS - RELIABILITY GROWTH TESTING

Richard Wisniewski, Reliability Information Analysis Center

In the early stages of new product development, problems exist in the design and manufacturing processes that negatively impact reliability. If uncorrected, these deficiencies would likely manifest themselves in field use, resulting in equipment down-time, increased maintenance costs, increased safety and liability exposure, and dissatisfied customers.

Reliability growth is the result of an iterative process of failure mode identification and mitigation. As a design or process matures, it is investigated to identify actual or potential sources of failures and their accelerating mechanisms. Further effort is then spent on eliminating or reducing the impact of these problem areas. The effort can be applied to system design, manufacturing process design, or any of the processes that support them.

This article briefly describes three types of reliability growth tests, and the techniques that are most commonly used to model the results. The Reliability Growth Testing (RGT) modeling techniques are then illustrated using numerical examples from a sample case study. For more detailed information on the topic of reliability growth, the reader is encouraged to consult the references listed at the conclusion of this article.

Reliability Growth Testing

Formal RGT is performed to evaluate current reliability, identify and eliminate hardware defects and software faults, and forecast future product or system reliability. Reliability metrics are compared to planned, intermediate goals to assess progress. Depending on the achieved progress (or lack thereof), resources can be allocated (or reallocated) to meet those goals in a timely and cost-effective manner.

Test-Fix-Test

In an absolutely pure **test-fix-test** program, testing stops when a failure is observed and does not resume until a design (or process) change is implemented on the system under test. When the testing resumes, it is with a system that presumably has incrementally better reliability. In most cases this type of program is impractical, as testing is likely to continue with a repair, and the fix will be implemented later. Nevertheless, if fixes are inserted as soon as possible, and while testing is still proceeding, the reliability will increase in a step-wise fashion as the causes of the individual failures are corrected (see Figure 1). Continuing to test after the fix is inserted will serve to verify the effectiveness of the design change.

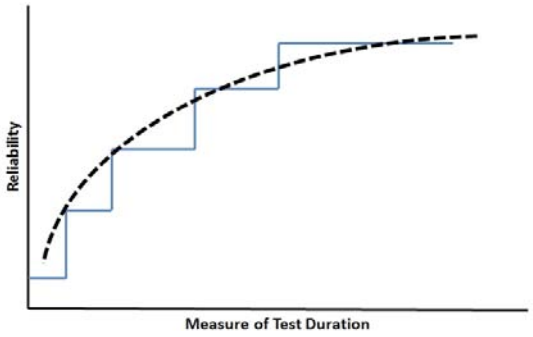

Figure 1 - Graph of Reliability in a Test-Fix-Test Program

continued on next page ›››

continued from page 13

Test-Find-Test

During a **test-find-test** program, design fixes are not incorporated into the system until the end of the test phase (but before the start of the next testing period). Since a large number of fixes will generally be incorporated into the system at the same time, there is usually a significant jump in system reliability at the end of a test phase. The fixes incorporated into the system between test phases are called delayed fixes (see Figure 2).

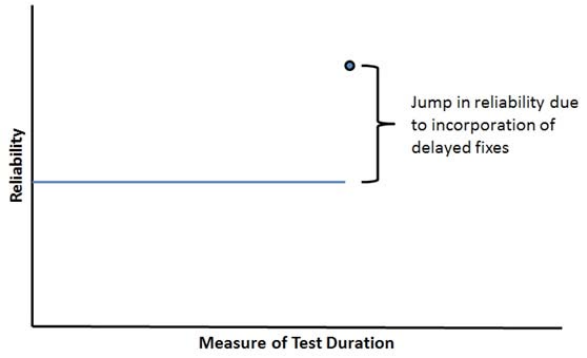

Figure 2 - Graph of Reliability in a Test-Find-Test Program

Test-Fix-Test with Delayed Fixes (including Test-Fix-Find-Test)

The test program commonly used in development testing employs a combination of the two types of fix insertions discussed above. In this case, some fixes are incorporated into the system during the test, while other fixes are delayed until the completion of the test phase. Consequently, system reliability improvement will generally be seen as a smooth process during the test phase, and then jump due to the insertion of the delayed fixes.

Reliability Growth Models

Reliability growth models can be generalized into three basic types: planning, tracking and projection. While many different variants have been developed, the Duane, Crow-AMSAA, and Crow Extended models are three of the most commonly used methods for reliability growth planning and tracking. Each of these methods will be briefly described and illustrated below.

Duane Model

The Duane reliability growth model assumes that a plot of the log of the cumulative MTBF vs. log of cumulative test time is a straight line, the slope of which represents the growth rate. The growth rate is a measure of how quickly and efficiently failure modes are being discovered and removed from the design. A guide relating a growth rate to the execution of an RGT program is shown in Table 1. The growth rate for most projects averages between 0.25 and 0.4. The upper limit on the growth rate is 0.6, and growth rates above 0.5 are rare.

Table 1 - Duane Reliability Growth Rates

Growth Rate	Comment
0.4 to 0.6	A top priority program is in effect to discover and eliminate failure modes. Immediate attention, corrective action development and implementation prevail.
0.3 to 0.4	An above average reliability growth program exists. A well-managed plan and action on important failure modes is typical.
0.2 to 0.3	Routine attention is paid to reliability improvement. Environmental testing may not be performed. Action taken on important failure modes only.
0.1 to 0.2	Reliability improvement is given low priority. Only the most critical failure modes may be addressed.

Mathematically, the Duane model can be represented by:

$$MTBF_C = MTBF_0 \left(\frac{T}{T_0}\right)^{\alpha} \quad \text{and} \quad MTBF_I = {}^{MTBF_C}/_{(1-\alpha)}$$

where "T" is the test time, "T_0" is the time at the beginning of the monitoring period (initial time interval), "$MTBF_0$" is the average initial MTBF over the initial time interval, "$MTBF_C$" is the cumulative MTBF at time "T", "$MTBF_I$" is the instantaneous MTBF (mathematical representation of the MTBF if all previous failure occurrences are corrected) at time "T", and "α" is the growth rate.

A plot of the log of the instantaneous MTBF vs. log of cumulative test time will also be a straight line and will be parallel to the cumulative MTBF plot. The RGT will proceed until the instantaneous MTBF reaches the MTBF goal. This resulting plot is known as the **idealized growth curve**.

The Duane model is often used to plan a reliability growth test. For example, consider the data provided in Table 2 for a proposed RGT for a Signal Processing Computer (SPC).

Table 2 - Sample Reliability Growth Test Parameters

Parameter	Symbol	Value (hours)
MTBF Goal	$MTBF_I$	200
Initial MTBF (Average over 1st Test Phase)	$MTBF_0$	50
Length of 1st Test Phase	T_0	100
Length of Test	T	2,000

Applying the Duane model, the growth rate parameter "α" necessary to support the reliability growth program defined in Table 2 is calculated as the solution to:

$$\log\left(\frac{MTBF_I}{MTBF_0}\right) = \alpha \log\left(\frac{T}{T_0}\right) - \log(1-\alpha)$$

Substituting we have:

$$\log\left(\frac{200}{50}\right) = \alpha \log\left(\frac{2{,}000}{100}\right) - \log(1-\alpha)$$

Solving the equation iteratively, we find that the growth rate necessary to support the goals of the RGT is:

$$\alpha \approx 0.33$$

The resulting idealized growth curve is provided in Figure 3.

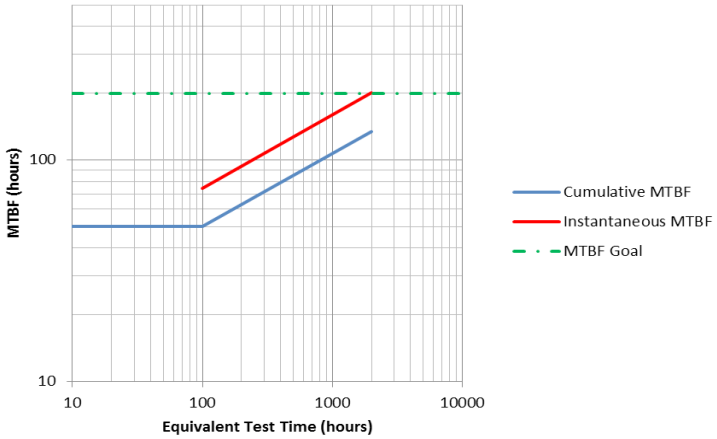

Figure 3 – RGT Idealized Growth Curve - Duane

Plotting the actual failure data obtained during the RGT on a graph similar to that shown in Figure 3 will indicate if the actual growth rate will be sufficient to support the MTBF goal in the desired time frame. If the growth rate is insufficient, additional measures such as increasing the efficiency at which corrective actions are introduced, increasing the effectiveness of corrective actions or increasing the stress level of the test to speed the precipitation of failure modes may be necessary.

As an alternative to the continuous approach, an RGT can be divided into test phases and corrective actions incorporated at the end of each phase. For example, suppose it was decided to divide the RGT into five test phases of lengths as shown in Table 3. The average number of failures and average MTBF can then be estimated for each test phase. The average number of failures occurring in phase "i" is estimated from the difference, "H_i", between the total number of failures occurring through the "i^{th}" phase, "$N(t_i)$" and the "$(i\text{-}1)^{th}$" phase, "$N(t_{i-1})$":

$$H_i = N(t_i) - N(t_{i-1})$$

$$N(t_i) = (\lambda_I)(t_I)\left(\frac{t_i}{t_I}\right)^{(1-\alpha)}$$

where "λ_I" is the average failure rate over the initial phase, "t_I" is the length of the initial phase and "t_i" is the cumulative time at the completion of the "i^{th}" phase. For example, if the length of the second phase is 300 hours, then using the average failure rate over the initial test phase and length of the initial phase as described in Table 3 we can calculate the following:

$$N(t_2) = (0.02)(100)\left(\frac{400}{100}\right)^{(1-0.33)} = 5.1$$

$$N(t_1) = (0.02)(100)\left(\frac{100}{100}\right)^{(1-0.33)} = 2.0$$

The average number of failures occurring during the second phase is then estimated to be:

$$H_2 = N(t_2) - N(t_1) = 5.1 - 2.0 = 3.1$$

The average MTBF over the second phase is estimated to be:

$$MTBF_2 = \frac{length\ of\ phase\ 2}{H_2} = \frac{300}{3.1} = 96.8\ hours$$

The average number of failures and MTBF over each of the planned test phases is summarized in Table 3.

Table 3 - Estimated Average Number of Failures and MTBF by Test Phase

Test Phase (i)	Cumulative Number of Failures ($N(t_i)$)	Avg. Number of Failures in Test Phase (H_i)	Test Phase Start-End (hours)	Test Phase Duration (hours)	Cumulative Test Time at Conclusion of Phase (t_i)	Avg. MTBF Over Test Phase ($MTBF_i$)
1	2	2	0-100	100	100	50
2	5.1	3.1	100-400	300	400	97
3	8.1	3.0	400-800	400	800	133
4	11.7	3.6	800-1,400	600	1,400	167
5	14.9	3.2	1,400-2,000	600	2,000	188

continued on next page ›››

continued from page 15

The average MTBF by test phase is shown in Figure 4. Since corrective actions are incorporated between test phases, the MTBF within a test phase remains constant, and a step-wise MTBF jump occurs at the start of the next phase. A comparison of the actual vs. expected number of failures within a test phase will indicate if the RGT is proceeding according to plan.

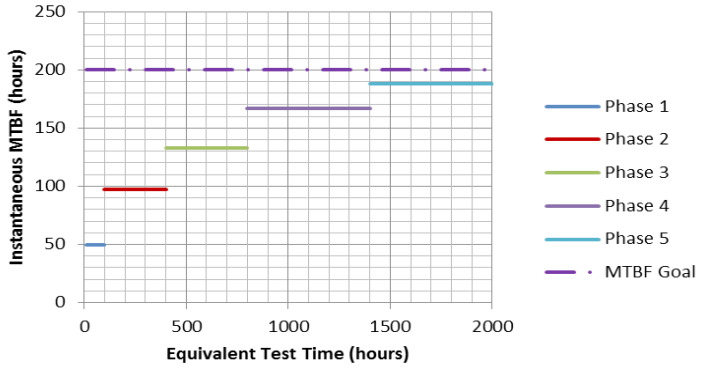

Figure 4 – RGT Planned Growth Curve - Duane

Crow-AMSAA Model

The Crow-AMSAA model (called the Reliability Growth Tracking Model – Continuous in MIL-HDBK-189) employs the Weibull process to track and model reliability growth that occurs from the introduction of design fixes during a development test phase. It does not address the growth that occurs as a result of delayed fixes at the end of test phase.

The Crow-AMSAA model allows the engineer to estimate the instantaneous failure rate (and, hence, MTBF) based upon a demonstrated cumulative failure rate pattern within a test phase. It assumes that failures within a test phase follow a non-homogeneous Poisson process (NHPP), and that the instantaneous failure rate can be approximated with a Weibull intensity function. Mathematically, the Crow-AMSAA model can be represented by:

$$\rho(t) = \lambda \cdot \beta \cdot t^{(\beta-1)} \quad \text{and} \quad MTBF_I = {}^{1}/_{\rho(t)}$$

where "ρ(t)" is the instantaneous failure rate at time "t", "$MTBF_I$" is the instantaneous MTBF at time "t", "β" is the shape parameter, and "λ" is the scale parameter. "β < 1" implies that reliability growth is occurring (decreasing failure rate); "β > 1" implies that deterioration is occurring (increasing failure rate); and "β = 0" implies no growth (constant failure rate).

The Crow-AMSAA shape and scale parameters are calculated as follows:

$$\hat{\beta} = \frac{F}{F \ln T - \sum_{i=1}^{F} \ln X_i} \quad \text{and} \quad \hat{\lambda} = \frac{F}{T^{\hat{\beta}}}$$

where "F" is the total number of failures at time "T", "X_i" is the equivalent cumulative equipment operating hours at the time of the "i^{th}" failure, and "T" is the total equivalent test time at which the parameters are being calculated.

To illustrate the implementation of the Crow-AMSAA model, consider the sample RGT data for the SPC, as shown in Table 4. An asterisk denotes an SPC failure.

Table 4 - Sample Reliability Growth Test Data

Failure Number	Test Article #1 Hours	Test Article #2 Hours	Test Article #3 Hours	Test Article #4 Hours	Test Article #5 Hours	Cumulative Hours
1	14.3*	0	0	0	0	14.3
2	55.0*	19.2	0	0	0	74.2
3	88.4	21.5*	18.4	15.8	0	144.1
4	104.4*	44.6	21.3	21.7	31.9	223.9
5	149.5	69.2	32.0*	38.7	39.6	329.0
6	182.3	98.7*	75.4	51.2	49.8	457.4
7	214.2	149.7	121.5	64.6*	79.0	629.0
8	263.0	198.6	170.3	113.4	80.4*	825.7
9	288.1*	225.4	197.1	140.2	107.2	958.0
10	314.3	251.6	209.9*	166.4	133.5	1075.7
11	381.8	262.6*	277.3	233.9	200.9	1356.5
12	400.0	334.1	348.8	250.3*	272.5	1605.7
13	400.0	382.2	396.9	298.3	293.0*	1770.4
14	400.0	400.0	400.0	385.4*	400.0	1985.4
END	400.0	400.0	400.0	400.0	400.0	2000.0

*Indicates failure occurrence

Calculating the Crow-AMSAA parameters at the end of the test (T = 2,000 hours), we have:

$$\hat{\beta} = \frac{F}{F\ln T - \sum_{i=1}^{F}\ln X_i} = \frac{14}{14\ln(2000) - 85.9428} = 0.683929$$

$$\hat{\lambda} = \frac{F}{T^{\hat{\beta}}} = \frac{14}{2000^{0.683929}} = 0.077347$$

$$\widehat{\rho(T)} = \hat{\lambda}\hat{\beta}T^{(\hat{\beta}-1)} = (0.077347)(0.683929)(2000)^{(0.683929-1)} = 0.004788$$

$$\widehat{MTBF}(T) = \frac{1}{\hat{\rho}(T)} = \frac{1}{0.004788} = 208.8759\ hours \approx 208.88\ hours$$

From these calculations, it can be concluded that reliability growth is occurring ("β < 1"), and that the instantaneous MTBF at the end of the test is approximately 209 hours.

Using the upper and lower bound coefficient values found in Table VI in MIL-HDBK-189A, the 80% two-sided confidence interval for the MTBF at 2,000 hours is:

$$MTBF_{Lower} = L_{\gamma,F} \cdot \widehat{MTBF} = (0.604)(208.88) = 126.16\ hours$$

$$MTBF_{Upper} = U_{\gamma,F} \cdot \widehat{MTBF} = (1.846)(208.88) = 385.59\ hours$$

The final step is to test the Crow-AMSAA model goodness-of-fit. This is accomplished by calculating a Cramer-von Mises test statistic and comparing it to a critical value corresponding to a chosen significance level. The test statistic is calculated using the following equation:

$$C_F^2 = \frac{1}{12F} + \sum_{i=1}^{F}\left[\left(\frac{X_i}{T}\right)^{\bar{\beta}} - \frac{2i-1}{2F}\right]^2$$

where the unbiased estimator of "β" is $\bar{\beta} = \frac{F-1}{F}\hat{\beta}$.

At the end of the test (T=2,000 hours) we have:

$$\bar{\beta} = \frac{F-1}{F}\hat{\beta} = \frac{14-1}{14}(0.683929) = 0.635077$$

$$C_{14}^2 = \frac{1}{12F} + \sum_{i=1}^{F}\left[\left(\frac{X_i}{T}\right)^{\bar{\beta}} - \frac{2i-1}{2F}\right]^2 = \frac{1}{(12)(14)} + \sum_{i=1}^{14}\left[\left(\frac{X_i}{2000}\right)^{0.635077} - \frac{2i-1}{(2)(14)}\right]^2 = 0.013565$$

From Table VIII in MIL-HDBK-189A, the critical value for the Cramer-von Mises statistic at the 0.05 significance level is 0.214. Since the Cramer-von Mises statistic is less than the critical value, the Crow-AMSAA model is accepted as a good fit to the data.

Crow Extended Model

The Extended Reliability Growth Projection Model was developed by Crow to address the common and practical case where some corrective actions are incorporated during test and some corrective actions are delayed and incorporated at the end of the test (test-fix-find-test). In the application of the Crow Extended model, three types of failure modes are considered: "A" modes, which are those failure modes that will not receive corrective action; "BC" modes, which are those failure modes that will have corrective action incorporated during test; and "BD" modes, which are those failure modes whose corrective action is delayed until the end of the test (or test phase).

During a test phase, the corrective actions for the BC-modes influence the growth in the system reliability. At the end of a test phase, the incorporation of corrective actions for the BD-modes results in further reliability growth, typically as a discrete jump. Estimating this increased reliability with test-fix-find-test data is the objective of the Crow Extended Model.

The Crow Extended Model also introduces the concept of "fix effectiveness". Fix effectiveness is based upon the idea that corrective actions may not completely eliminate a failure mode and that some residual failure rate due a particular mode will remain. The "fix effectiveness factor" or "FEF" represents the fraction of a failure mode's failure rate that will be mitigated by a corrective action. An FEF of 1.0 represents a "perfect" corrective action; while an FEF of 0 represents a completely ineffective corrective action. History has shown that typical FEFs range from 0.6 to 0.8 for hardware and higher for software.

The estimate of the projected failure intensity for the Crow Extended Model at time "T" is:

$$\hat{\lambda}_{EM} = \hat{\lambda}_{CA} - \hat{\lambda}_{BD} + \sum_{j=1}^{M}(1-d_j)\frac{N_j}{T} + \bar{d}\hat{h}(T|BD)$$

In this equation, "λ_{CA}" is the demonstrated failure rate at the end of a test phase, which accounts for the incorporation of corrective actions for BC modes; "λ_{BD}" is the constant failure intensity for the BD modes; the summation term (where "M" is the number of distinct BD modes, "N_j" is the number of occurrences of the j^{th} BD mode and "d_j" is the FEF for the j^{th} BD mode) is the residual failure intensity of the observed BD modes; and "h(T | BD)" is the first occurrence function for the BD modes ("d" is the mean FEF of the BD modes).

In order to illustrate the application of the Crow Extended model consider the failure data provided in Table 4 for the Crow-AMSAA model. Furthermore, suppose that failure mode type identification is as shown in Table 5.

Table 5 - Sample RGT Data for the Crow Extended Model

Failure Number	Failure Mode Type	Cumulative Failure Time (X_i)	ln(T/Xi)
1	BD1	14.3	4.940643
2	BC1	74.2	3.294138
3	BC2	144.1	2.630395
4	BD1	223.9	2.189703
5	BD1	329.0	1.804845
6	BD2	457.4	1.475344
7	A	629.0	1.156771
8	BD1	825.7	0.884671
9	BD1	958.0	0.736055
10	BC3	1075.7	0.620176
11	BD2	1356.5	0.388239
12	BD1	1605.7	0.219587
13	A	1770.4	0.121942
14	BD3	1985.4	0.007327
Sum			20.46984

continued on next page ›››

continued from page 17

We begin by calculating "λ_{CA}", which is the failure rate for the Crow-AMSAA model and is based upon the entire dataset:

$$\hat{\lambda}_{CA} = \hat{\lambda}\bar{\beta}T^{(1-\bar{\beta})}$$

The unbiased estimator for the shape parameter is calculated as:

$$\bar{\beta} = \frac{N-1}{\sum_{i=1}^{N}\ln\left(\frac{X_i}{T}\right)} = \frac{14-1}{20.46984} = 0.635081$$

The scale parameter is calculated as:

$$\hat{\lambda} = \frac{N}{T^{\bar{\beta}}} = 0.112126$$

Substituting,

$$\hat{\lambda}_{CA} = \hat{\lambda}\bar{\beta}T^{(1-\bar{\beta})} = (0.112126)(0.635081)(2000)^{(1-0.635081)} = 0.004446$$

Next, we consider the BD modes as shown in Table 6.

Table 6 - Sample RGT Data for Crow Extended Model – BD Modes

Failure Number	Time to First Failure (X_j)	Number of Occurrences (N_j)	Nominal FEF (d_j)	ln(T/Xj)	$(1-d_j)*N_j/T$
BD1	14.3	6	0.7	4.940643	0.0009
BD2	457.4	2	0.8	1.475344	0.0002
BD3	1985.4	1	0.75	0.007327	0.000125
Sum	**M = 3 (3 distinct BD modes)**	**9**	**2.25**	**6.423314**	**0.001225**

The constant failure intensity for the BD modes is calculated:

$$\hat{\lambda}_{BD} = \frac{\sum_{j=1}^{M} N_j}{T} = \frac{9}{2000} = 0.0045$$

From Table 6, the summation term is shown to be:

$$\sum_{j=1}^{M}(1-d_j)\left(\frac{N_j}{T}\right) = 0.001225$$

The average FEF is calculated as:

$$\bar{d} = \frac{\sum_{j=1}^{M} d_j}{M} = \frac{2.25}{3} = 0.75$$

The first occurrence function for the BD modes is calculated as:

$$h(T|BD) = \hat{\lambda}\bar{\beta}T^{(1-\bar{\beta})}$$

where the parameters are calculated from the BD mode data shown in Table 6:

$$\bar{\beta} = \frac{M-1}{\sum_{j=1}^{M}\ln\left(\frac{X_j}{T}\right)} = \frac{3-1}{6.423314} = 0.311366$$

$$\hat{\lambda} = \frac{M}{T^{\bar{\beta}}} = 0.28138$$

$$h(T|BD) = \hat{\lambda}\bar{\beta}T^{(1-\bar{\beta})} = (0.28138)(0.311366)(2000)^{(1-0.311366)} = 0.000467$$

The projected failure rate and MTBF at the start of the next test phase after incorporation of corrective actions for the BD modes can then be calculated from the Crow Extended Model as follows:

In summary, based on the Extended Model estimates, the MTBF grew to 224.95 hours (from $MTBF_{CA}=1/\lambda_{CA}$) as a result of corrective actions for BC failure modes during the test, and then jumped to 657.53 hours as a result of the delayed corrective actions after the test for the three distinct BD failure modes.

Summary

The discussion presented here provides the reader with an illustration as to how reliability growth planning, tracking and projection models can be used to quantify the improvement in reliability that occurs during an RGT, regardless of the corrective action implementation strategy. For further information pertaining to the Duane, Crow-AMSAA and Crow Extended models, as well as other RGT modeling methodologies, the reader is referred to MIL-HDBK-189C.

References

1. MIL-HDBK-189C "Reliability Growth Management", 14 June 2011
2. Nicholls, D. (Editor), "System Reliability Toolkit", Reliability Information Analysis Center, 2005
3. Nicholls, D., P. Lein, T. McGibbon, "Achieving System Reliability Growth Through Robust Design and Test", Reliability Information Analysis Center, 2011
4. Wisniewski, R., "Quanterion REL*ease* Series: Reliability Growth", Quanterion Solutions Incorporated, 2012

NANO NEW YORK

Alex MacDiarmid, Quanterion Solutions

Abstract

The average consumer eagerly awaits the release of the latest smartphone or tablet, often unaware of the underlying technology responsible for new and improved capabilities. Meanwhile, semiconductor manufacturers continue to innovate, developing cutting-edge technologies to deposit and selectively remove materials from the wafer surface, scaling electronic components to ever-smaller dimensions. This prolonged period of innovation is the result of a great deal of both public and private investment, including partnerships such as those developed in New York State. These collaborative consortiums, in addition to the involvement of government-sponsored Information Analysis Centers (IACs) and R&D laboratories should allow for the continuation of Moore's Law into the foreseeable future.

Nanotechnology

Nanotechnology, the application or manipulation of technologies at the molecular or atomic level, is one of the buzzwords that seems to have garnered the most interest and discussion in the science and technology (S&T) community. Generally defined, it can refer to nearly any technology involving very small components or related to a material's physical structure ($1x10^9$ nanometers (nm) = 1 meter). However, the field that it is probably most often associated with is the design and fabrication of Nanoelectronic devices, as this industry has developed many of the processes and techniques for the manipulation of materials at the nanoscale.

The traditional approach to the continuation of Moore's Law has predominantly consisted of component scaling efforts. Over the course of time, however, these efforts have been so successful that the industry is rapidly approaching the physical limitations of component materials, to the point where dimensions may soon be measured in units of atoms. Even if the capability to fabricate components of this size is achieved, the performance and reliability of these devices must be considered in the feasibility of such designs.

In light of these circumstances, an alternative approach to smaller, more powerful electronics involves advanced packaging techniques. Packaging is arguably as important as processing, since the package mechanically supports the die, connects it to the external world and provides protection from internal stresses (e.g., thermal cycling) and external contaminants. This decades-old approach to fitting more components into a smaller space has progressed over the years from simplistic 2-dimensional arrangements like the Multichip Module (MCM), to more advanced designs like the System in Package (SiP), Package on Package (PoP) and 3D chip stacking and integration concepts.

Image (Top): Rendering of the Computer Chip Commercialization Center (Quad-C) facility currently under construction at the SUNYIT campus (SUNYIT)

continued on next page ›››

continued from page 19

The reliability of these packages continues to be an important topic of study in this industry. More specifically, the close proximity of multiple die often causes issues with the removal of heat, a frequently cited root cause of numerous electronic failure mechanisms. Nonetheless, these technologies continue to be pursued because they produce unparalleled achievements in the size, speed and computing power of electronic devices. The subsequent reductions in the size and weight of electronic equipment yield numerous benefits to Department of Defense (DoD) applications. From the growing cache of infantryman electronics (e.g., communications, GPS, wearable computers) to supercomputers, flight controls and munitions guidance systems, the implementation of new electronics technologies will undoubtedly allow the DoD to realize significantly capability improvements in future systems.

Information Analysis Centers (IACs)

The DoD's Information Analysis Centers (IACs) are Defense Technical Information Center (DTIC)-sponsored Centers of Excellence in specific S&T domains, providing valuable resources to the DoD community such as relevant Scientific and Technical Information (STI), topic-specific training, published handbooks/databooks and Subject Matter Expert (SME) analysis. The individual centers are not only tasked with collection, analysis and dissemination of STI, but must also possess a technical proficiency that allows them to provide responses to inquiries from the user community regarding specific topics in the IAC's scientific domain. This service helps various industries and government agencies to rapidly respond to new and emerging trends/threats/opportunities in a specific field.

At the Reliability Information Analysis Center (RIAC), electronics reliability is by no means a new topic of interest. The study of electronics-related failure mechanisms, as well as the collection and analysis of failure data to determine the rate at which they occur, has been ongoing for decades. However, with the continuing trend of scaling devices to miniscule dimensions, and packaging components more closely to one another, new failure mechanisms are manifesting themselves in these devices; especially as materials exhibit different behavior when thicknesses approach nanoscale dimensions. Accordingly, there are a number of reliability concerns regarding the future of electronic devices.

The RIAC SMEs at Quanterion Solutions are currently engaged in multiple Nanotech efforts, including a state-of-the-art report (SOAR) on electronics packaging techniques that describes both the benefits and disadvantages of each approach, as it relates to throughput, design and fabrication costs and device performance and reliability. The RIAC is also engaged with multiple New York State (NYS) Nanotech initiatives (described in greater detail in the following section), in an effort to collaborate with the manufacturing consortiums to leverage the RIAC SME's data collection and analysis capabilities.

NYS NANO

With the growing demand and dependence on personal computers, handheld devices and other digital sensors/controls, modern electronics have become engrained into our everyday lives. Accordingly, it's no wonder that this industry has been, and continues to be, the recipient of enormous public and private investment. Such is the case in upstate NY, where Governor Andrew Cuomo recently announced a $1.5 billion dollar public-private partnership to establish the state's second major hub for nanotechnology research and development. The initiative will bring six world-class technology companies to the center, headquartered at the College of Nanoscale Science and Engineering-State University of New York Institute of Technology (CNSE-SUNYIT) Computer Chip Commercialization Center (Quad-C) on the SUNYIT campus in Marcy, NY.

Figure 1: Rendering of the Computer Chip Commercialization Center (Quad-C) facility currently under construction at the SUNYIT campus (SUNYIT)

The "Nano Utica" complex features the $125 million Quad-C facility, a 253,000 square-foot structure that includes a two-floor, state-of-the-art cleanroom occupying more than 56,000 square feet. This facility will host the consortium's cutting-edge research, addressing new and emerging processing and fabrication techniques for future Nanoelectronic devices. More specifically, researchers will investigate innovative electronics packaging techniques (e.g., 3-D packaging) as well as advanced lithography and metrology (for process control). Quanterion, which runs the day-to-day operations of the RIAC on the SUNYIT campus (SUNYIT is a RIAC team member), plans to relocate to the Quad-C facility upon its completion in 2014.

The state's commitment to Nano is by no means limited to the recent developments in central New York. In fact, the Nano Utica initiative marks the second of such partnerships in NYS, mirroring SUNY CNSE's state-of-the-art NanoTech complex in Albany. Similar efforts are also underway in Syracuse, NY, where the Nanotechnology Innovation and Commercialization Excelerator (NICE) is hosted at the Lockheed Martin facility near the NYS Thruway. The Nanotech College has also requested proposals from developers in the Buffalo Niagara region for the development of an economic hub for Nanotech research, workforce training and manufacturing. The former

Infotonics Technology Center in Canandaigua, NY has also merged with the CSNE, and now provides a facility where the technologies developed in Albany can be employed. With all of this investment and collaboration across the state, New York is positioning itself to become the "Silicon Valley" of the 21st century.

NYS S&T Centers

While the recent Nanotechnology developments provide an outstanding opportunity for upstate NY, the state also provides a number of excellent resources in relevant scientific fields. In addition to the RIAC, NYS is also home to three additional IACs with a technical focus related to electronics manufacturing, performance and/or longevity, as well as practical applications for the DoD. These centers include the Cybersecurity and Information Systems IAC (CSIAC), the Advanced Materials, Manufacturing and Testing IAC (AMMTIAC) and the Weapons Systems Technology IAC (WSTIAC). In 2014 three of the four NYS IACs (RIAC, AMMTIAC and WSTIAC) will be consolidated into the Defense Systems IAC (DSIAC).

Another example is the Air Force Research Laboratory's Information Directorate (AFRL RI) located in Rome, NY. Less than two hours from Albany and only a short drive from SUNYIT's Quad-C facility, AFRL RI hosts more than 800 military and civilian scientists and engineers performing state-of-the-art research in Cyber Science Technology, Processing and Exploitation, Connectivity and Dissemination and Autonomy, Command and Control, and Decision Support.

Figure 2: AFRL RI in Rome, NY – The Sherwood Boehlert Center of Excellence for Information Science and Technology

AFRL has long-standing history in the electronics field, dating back to its establishment in 1950 as the Air Force Electronics Center. Over the years, the center has seen various derivatives of its name (the Rome Air Development Center, Rome Laboratory), but its focus on electronics, communications and information systems has remained.

Nano at AFRL

As a research laboratory, AFRL RI is not only affected by recent developments in the electronics field, but also very much engaged in the ongoing R&D. For instance, projects like the Crossbar Nanocomputer and the Quantum Information Science Facility address the feasibility of different nanoscale designs through the evaluation of material properties and fabrication technologies. The analysis not only considers whether a specific size, level of precision, or performance metric can be achieved, but also the throughput, associated production (or acquisition) costs and complexity of design, as well as any potential deleterious effects on the device's performance or reliability.

Another aspect of AFRL RI's current project work is the attempt to bridge the gap between nanoscale electronic devices and the approaches and techniques to ensure the security of the information stored on, or accessed by, those devices. The so-called "bring cyber to Nano" approach of integrating cybersecurity with Nanoelectronic design, fabrication and/or packaging has the potential to provide a considerable benefit to the reliability and security of these devices.

AFRL RI is pursuing these R&D efforts both individually and in collaboration with other research organizations and academic institutions. They currently have an Educational Partnership Agreement (EPA) in place with SUNY CNSE's Albany Nanotech Complex, the $14 billion nanofabrication facility that is the model for New York State's public-private partnership for technological innovation. Their efforts at CSNE primarily include the fabrication of hybrid CMOS/Memristor Nanoelectronic circuits, and the Secure Cyber Key development and AES Encryption. Similar partnerships with Union College are investigating the use of carbon nanotubes (CNTs) for high density interconnects.

Summary

The magnitude of the public-private investment in Nanotech is without precedent, and the State of New York is poised to be the epicenter of this technological innovation. The improvements associated with the progression towards nanoscale devices extend well beyond consumer convenience. Smaller devices occupy a smaller footprint, which, combined with their reduced power consumption (smaller power sources (e.g., battery)), can produce considerable weight and space savings. More importantly, they operate at higher speeds and provide greater computing power. These are the fundamental improvements that allow for the conceptual devices of the future to become a reality. The developments at these and other Nanotech centers are the necessary R&D that will allow the DoD to maintain its technical superiority both on the battlefield, and in cyberspace.

FUTURE EVENTS IN RMQSI

JANUARY

S	M	T	W	T	F	S
			1	2	3	4
5	6	7	8	9	10	11
12	13	14	15	16	17	18
19	20	21	22	23	24	25
26	27	28	29	30	31	

FEBRUARY

S	M	T	W	T	F	S
						1
2	3	4	5	6	7	8
9	10	11	12	13	14	15
16	17	18	19	20	21	22
23	24	25	26	27	28	

MARCH

S	M	T	W	T	F	S
						1
2	3	4	5	6	7	8
9	10	11	12	13	14	15
16	17	18	19	20	21	22
23	24	25	26	27	28	29
30	31					

APRIL

S	M	T	W	T	F	S
		1	2	3	4	5
6	7	8	9	10	11	12
13	14	15	16	17	18	19
20	21	22	23	24	25	26
27	28	29	30			

MAY

S	M	T	W	T	F	S
				1	2	3
4	5	6	7	8	9	10
11	12	13	14	15	16	17
18	19	20	21	22	23	24
25	26	27	28	29	30	31

JUNE

S	M	T	W	T	F	S
1	2	3	4	5	6	7
8	9	10	11	12	13	14
15	16	17	18	19	20	21
22	23	24	25	26	27	28
29	30					

JANUARY 2014

2014 Annual Reliability and Maintainability Symposium
Colorado Springs, CO
January 27, 2014 thru January 30 2014
Contact: RAMS // http://rams.org/contact/

FEBRUARY 2014

2014 International Conference on Reliability Optimization and Information Technology (ICROIT)
Haryana, India
February 6, 2014 thru February 8, 2014
Contact: Dr. S. S. Tyagi // P: 9810484802 // shyam.fet@mriu.edu.in // http://icroit2012.org/

The Seventh International Conference on Communication Theory, Reliability, and Quality of Service
Nice, France
February 23, 2014 thru February 27, 2014
Contact: http://www.iaria.org/conferences2013/CTRQ13.html

MARCH 2014

The International Symposium on Quality Electronic Design (ISQED)
Santa Clara, CA
March 10, 2014 thru March 12, 2014
Contact: ISQED // P: 408.436.3000 // F: 408.573.0200 // eFAX: 408.516.8228 // isqed2013@isqed.org // http://www.isqed.org/

12th Annual Conference on Systems Engineering Research (CSER)
Redondo Beach, CA
March 21, 2014 thru March 22, 2014
Contact: cser2014@incose-la.org // http://www.incose-la.org/events/conferences/cser-2014-welcome.html

26th Annual IEEE Software Technology Conference
Long Beach, CA
March 29, 2014 thru April 3, 2014
Contact: cps@computer.org // http://ieee-stc.org/index.html

APRIL 2014

Reliability 2.0 High Performance Reliability Management
Las Vegas, NV
April 7, 2014 thru April 11, 2014
Contact: http://maintenanceconference.com/r2/

15th Annual Conference and Exhibition – Reliable Plant 2014
San Antonio, TX
April 22, 2014 thru April 24, 2014
Contact: Jason Sowards // jsowards@noria.com

Systems Engineering and Test and Evaluation Conference - SETE2014
Adelaide, Australia
April 28, 2014 through April 30, 2014
Contact: sapro // P: +08 8274.6048 // F: +08 8274.6000 // sete@sapmea.asn.au // http://www.sapmea.asn.au/conventions/sete2014/index.html

MAY 2014

ESTECH 2014
San Antonio, TX
May 13, 2014 thru May 16, 2014
Contact: Heather Wooden // P 847. 981.0100, ext. 20 // marketing@iest.org // http://www.iest.org/Sponsorship/Exhibit/ESTECH-2014

2014 IEEE International Workshop Technical Committee on Communications Quality and Reliability (CQR 2014)
Tucson, AZ
May 18, 2014 thru May 23, 2014
Contact: Kevin Krantz // P: 972-583-2250 // Kevin.krantz@ericsson.com

JUNE 2014

2014 IEEE International Reliability Physics Symposium (IRPS)
Waikoloa, HI
June 1, 2014 thru June 5, 2014
Contact: David Barber // P: 828.898.7001 // F: 828.898.6375 // dbarbsta@aol.com // http://www.irps.org/

International Applied Reliability Symposium
Indianapolis, IN
June 3, 2014 thru June 5, 2014
Contact: ReliaSoft // P 888.886.0410 or 520.886.0410 // info@ARSymposium.org // http://www.arsymposium.org/northamerica/index.htm

2014 IEEE International Conference on Prognostics and Health Management
Spokane, WA
June 22, 2014 thru June 25, 2014
Contact: http://phmconf.org/Committees.htm

Mega Rust 2014: U.S. Navy Corrosion Conference
San Diego, CA
June 24, 2014 thru June 26, 2014
Contact: Mike Huling // P 703.597.4225 // mhuling@navalengineers.org // https://www.navalengineers.org/events/individualeventwebsites/Pages/MegaRust2014.aspx

2014 IEEE 21st International Symposium on the Physical and Failure Analysis of Integrated Circuits (IPFA)
Singapore
June 30, 2014 thru July 4, 2014
Contact: Jasmine Leong // P: +065-67432523 // ieee_ipfa@singnet.com.sg

Please fax completed survey to
315.351.4209 – ATTN: Journal Editor

RIAC JOURNAL SURVEY

DECEMBER 2013

Journal Format ☑ Hard Copy ☐ Web Download

How satisfied are you with the **content** (article technical quality) in *this issue* of the Journal?

☐ Very Satisfied ☐ Satisfied ☐ Neutral ☐ Dissatisfied ☐ Very Dissatisfied

How satisfied are you with the **appearance** (layout, readability) of *this issue* of the Journal?

☐ Very Satisfied ☐ Satisfied ☐ Neutral ☐ Dissatisfied ☐ Very Dissatisfied

How satisfied are you with the **overall quality** of *this issue* of the Journal (compared to similar magazines, newsletters, etc.)?

☐ Very Satisfied ☐ Satisfied ☐ Neutral ☐ Dissatisfied ☐ Very Dissatisfied

How did you become **aware** of *this issue* of the Journal?

☐ Subscribe ☐ Colleague ☐ Library ☐ RIAC Website ☐ RIAC Email ☐ Conference/Trade Show

Would you **recommend** the RIAC Journal to a colleague?

☐ Definitely ☐ Probably ☐ Not Sure ☐ Probably Not ☐ Definitely Not

Please suggest general **changes / improvements** to the RIAC Journal that would improve your level of satisfaction:

Please suggest further **topics** for the RIAC Journal that might help it to better meet your needs:

Overall satisfaction

☐ Very Satisfied (5) ☐ Satisfied (4) ☐ Neutral (3) ☐ Dissatisfied (2) ☐ Very Dissatisfied (1)

CONTACT INFORMATION (OPTIONAL)

Name Position/Title

Organization Office Symbol

Address City State Zip

Country Email

Phone Fax

My Organization is: ☐ Army ☐ Navy ☐ Air Force ☐ Other DoD/Government ☐ Industry ☐ Academic ☐ Other

I need help with a reliability, maintainability, quality, supportability, or interoperability problem. ☐ Please contact me

Reliability Information Analysis Center
100 Seymour Road | Suite C101 | Utica, NY 13502-1311

THE RIAC ONLINE

- The RIAC's "Desk Reference" is a Virtual Knowledge Base of reliability know-how on best practices, analyses and test approaches.
- Save time and money at the RIAC's online store where you can browse, order, and immediately download electronic versions of most of the RIAC's products.

- Online Product Store
- RMQSI Library
- Technical Answers
- The RIAC Journal
- Upcoming Training Courses
- What's New at RIAC